Check for updates

The synthesis of graphene-based antioxidants to promote anti-thermal properties of styrene-butadiene rubber

Junjun Zhou, Laiyun Wei, Haitao Wei, Jing Zheng* and Guangsu Huang [iD] *

In this work, graphene oxide (GO) was functionalized with the reactive antioxidant intermediate 4-aminodiphenylamine (RT) to obtain the immobile antioxidant (GO-RT). Then the GO-RT was used as a filler to prepare styrene-butadiene rubber (SBR) composites for enhancing the thermal oxidative stability. The results of fourier transform infrared spectroscopy (FTIR), energy dispersive X-ray spectrometry (EDS), X-ray diffraction (XRD) and Raman spectroscopy demonstrated that RT has been successfully grafted onto the GO. The grafting efficiency of GO-RT was evaluated by thermogravimetric analysis (TGA). Oxidation induction time (OIT) tests, electron paramagnetic resonance (EPR) and accelerated aging tests revealed that GO-RT presented much better anti-oxidative and anti-migratory efficiencies than the corresponding low molecular counterpart (4010NA). Additionally, the mechanical strength of the modified rubber composites was also improved by the GO-RT. Thus, the GO-RT antioxidant has the excellent ability to improve the thermal oxidation resistance of SBR and also could obviously strengthen SBR.

1 Introduction

Diolefin elastomers, like natural rubber and styrene-butadiene rubber (SBR), are the most important rubbers and represent the largest consumption of elastomers in the world due to their many excellent properties in different fields.[1] However, diolefin elastomers easily undergo thermal oxidation due to the instability of unsaturated double bonds and active allylic hydrogens when exposed to thermal, oxidative or radiant conditions, which results in the scission of polymer chains and formation of extra crosslinks and oxygenic groups.[2,3] These reactions lead to a significant reduction of the mechanical properties of the SBR, and eventually shortened service life of the materials. Therefore, the research about how to reduce thermal oxidation to prolong their lifetime is vital for the rubber industry.

To delay the aging of diolefin elastomers, the antioxidant, such as the low molecular weight antioxidant with aromatic amines and aminophenol moieties, was commonly added into the elastomers to capture free radicals.[4-6] However, such low molecular weight antioxidants were easily migrated from the rubbers, which would reduce the anti-aging efficiency and pollute the environment at the same time.[7-10] Furthermore, excessive antioxidants would aggregate on the surface of rubbers, resulting in the decrease of mechanical strength and aging resistance of the rubbers.[10-12] In order to eliminate the shortcoming of low molecular weight antioxidants,

College of Polymer Science and Engineering, Sichuan University, State Key Lab of Polymer Materials Engineering, Chengdu, China. E-mail: huangguangsu@scu.edu.cn

predecessors had put forward a variety of approaches, such as enlarging the molecular weight of antioxidant, grafting the antioxidant onto the rubber molecular chains and grafting the antioxidant onto the filler.[13-17] Among these methods, grafting the antioxidants onto the fillers is the optimal way to gain the anti-migratory efficiency antioxidants with less damage on the performance of the rubbers. Till now, many inorganic or organic materials had been used as matrixes to fabricate the anti-migratory efficiency antioxidants. For example, B. Zhong *et al.* grafted the *N*-1,3-dimethylbutyl-*N*′-phenyl-*p*-phenylenediamine (4020) onto the filler of the graphene oxide (GO), and found that the filler-based antioxidant can improve the thermal oxidation resistance of styrene-butadiene rubber, the antioxidant also had high efficiency of immobility. However, the thermal oxidation resistance of SBR composites are not improved significantly.[18]

Compared with common inorganic materials, GO has higher surface area, remarkable thermal and mechanical properties to modify polymeric materials. Furthermore, some studies had demonstrated that GO could enhance the mechanical strength of the rubbers.[1,19,20] Thus, in the present study, a new type of antioxidant was fabricated by grafting the RT onto the surface of GO (the filler of rubber) and was used to enhance the aging-resistance of SBR.

The GO was firstly reacted with KH-560 to gain the epoxy groups. Then 4-aminodiphenylamine (RT) was grafted onto the GO by the reaction between epoxy and amines to obtain the immobile antioxidant (GO-RT). Afterwards, the SBR/GO-RT composites were prepared *via* two-roll mill. The OIT test was

carried out to evaluate the thermal oxidation resistance of SBR composites. TGA and EPR were also used to evaluate the anti-oxidative efficiency. The mechanical properties of SBR composites were also evaluated by the tensile test.

2 Experimental

2.1 Materials

Highly-purified graphite flakes (99.99%) were purchased from Qingdao Ruisheng Graphite Company, (China). The silane coupling agent 3-glycidoxypropyltrimethoxysilane (KH-560, purity 98%, Aladdin) and the reactive antioxidant intermediate 4-aminodiphenylamine (RT, 98%, Aladdin), N,N-dimethyl formamide (DMF, AR, Kelong) and anhydrous alcohol (AR, Kelong) were used as received. SBR1502 was supplied by Lanzhou petrochemical company (China). N-isopropyl-N'-phenyl-4-phenylenediamine (4010NA), Stearic acid (SA), zinc oxide (ZnO), N-cyclohexyl-2-benzothiazole sulfonamide (CZ) and sulfur were of commercial grade.

2.2 Preparation of graphite oxide

GO was prepared from graphite flakes by Hummer's method. Briefly, the graphite flakes were firstly reacted with the mixed solution of $NaNO_3$, $KMnO_4$ and H_2SO_4 for 48h.[21] Then the solution was dispersed in water by ultrasonic treatment and centrifuged at 10 000 rpm for 15 min to remove un-exfoliated graphite. Afterwards, the solution was dialyzed, centrifugated and freezing dried to obtain GO.

2.3 Synthesis of GO-RT

The immobile antioxidant GO-RT was prepared by two-step method as illustrated in Fig. 1. 2 g GO was firstly dissolved in the DMF (200 mL) and treated by ultrasonic treatment for 2 h. Then 5 mL KH-560 was dropwise added into the solution and reacted at 120 °C for 5 h. Subsequently, 4 g RT was dissolved in the DMF (150 mL) and added into the solution. After stirring for 48 h at 120 °C, the solution was poured into alcohol to remove the excess RT and filtered to obtain the solid. Finally, the solid

was washed with ethyl alcohol, filtered and dried in a vacuum oven at 60 °C for 12 h to obtain GO-RT.

2.4 Preparation of GO-RT/SBR composites

The SBR composites were prepared via two-roll mill. Firstly, the raw SBR was plasticated on two-roll mill. Then SA, CZ, ZnO, GO and sulfur were added onto the mill and mixed with SBR matrix for 15 min at room temperature. After being placed for 24 h, the composites were vulcanized at 151 °C under 15 MPa for 40 min. Finally, the vulcanized rubber was tailored in an average thickness of 1 mm. The compositions of SBR composites are listed in Table 1.

2.5 Characterization

Fourier transform infrared spectra (FTIR) were recorded on a Perkin-Elmer System 2000 infrared spectrum analyzer with KBr pellets in the wave number range from 4000 to 400 cm^{-1}. The scanning was performed 32 times with a resolution of 4 cm^{-1}. Raman spectra was recorded by HORIBA Transmission Raman and the wavelength of laser light was 633 nm. X-ray diffraction (XRD) pattern was recorded by using Philips at room temperature. TGA was carried out on Mettler Toledo TGA/DSC 1 instrument to determine the organic content of GO-RT and to calculate the activation energy. The RT-silica was heated from room temperature up to 800 °C at a heating rate of 10 °C min^{-1} in nitrogen. The values of activation energy were calculated from three TG curves at different heating speeds of 5, 10 and 20 °C min^{-1} in air from 30 to 800 °C. Scanning electron microscopy (SEM) images were obtained on an Inspect F at 20 kV.

2.6 Aging resistance test

The thermal oxidation resistance of SBR composites was evaluated by OIT test, which was conducted by the DSC on a TA Q200 instrument according to the standard method (ISO 11357-6, 2002). The sample was held at 40 °C for 5 min with a nitrogen flow of 50 mL min^{-1} to remove the air and then the sample was heated with a heating speed of 10 °C min^{-1} to 160 °C
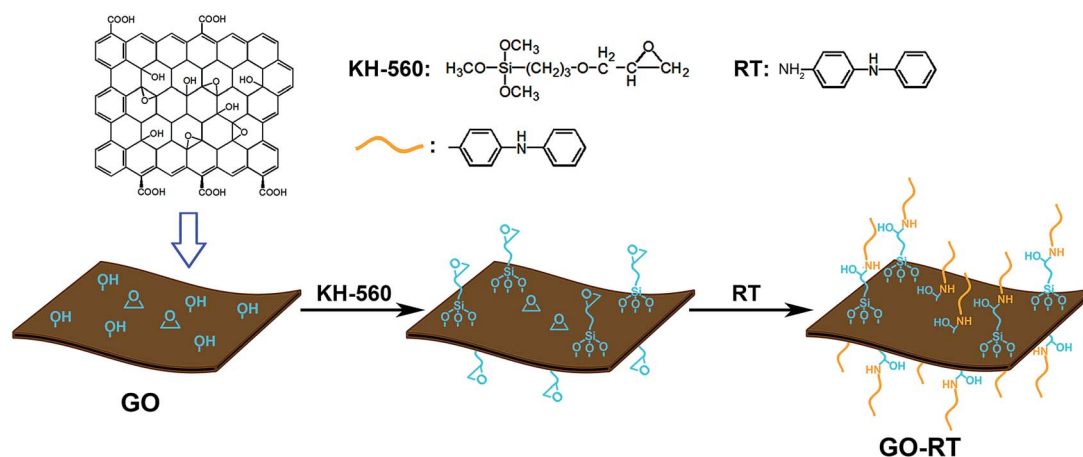

Fig. 1 Schematic illustration for the preparation of GO-RT.

Table 1 Composition of GO-RT/SBR composites[a]

	SBR	SBR/GO(4)/4010NA	SBR/GO-RT(1)	SBR/GO-RT(2)	SBR/GO-RT(3)	SBR/GO-RT(4)
SBR	100	100	100	100	100	100
GO	—	4	—	—	—	—
GO-RT	—	—	1	2	3	4
4010NA	0.15	0.6	—	—	—	—

[a] Rubber intergradient: zinc oxide (ZnO), 4 phr; stearic acid, 2 phr sulfur (S), 2 phr; *N*-cyclohexyl-2-benzothiazole sulfonamide (CZ), 1 phr.

maintained for another 5 min. Subsequently, nitrogen was replaced by oxygen at a flow rate of 50 mL min^{-1}. Then, an exothermic peak appeared resulting from the oxidation reaction of the SBR matrix, recording the time interval from oxygen flow to the F Instron 5567 material testing machine (with a 500 N load cell) was applied to measure the stress–strain curve at room temperature with extensional strain rate of 500 mm min^{-1} in accordance with the GB/T1040-92. The initial thickness and length of the samples were 1 and 15 mm, respectively. Each test chose an average value of five parallel samples. All samples for accelerated aging test were aged in air condition at 85 °C for different time.

Electron paramagnetic resonance (EPR) measurements were carried out on Bruker EPR EMX Plus (Bruker Beijing Science and Technology Ltd, USA) of a frequency 9.8 GHz approximately using a standard microwave power of 0.1 mW.

2.7 Extraction experiments

The SBR composites were immersed in deionized water at 50 °C by a thermostat water bath. After 48 h, the solutions were diluted and the absorbance at 220 nm were tested by a UV-vis spectrophotometer (shimadzu UV-1750). The concentrations of the solutions were calculated according to the standard curve.

### 2.8 Activation energy calculation

Thermal kinetic methods are commonly used to evaluate thermal properties of materials. In this work, Flynn–Wall–Ozawa method was used to calculate the activation energy during thermal oxidative by using the following equation:[22,23]

$$\log \beta = \log \frac{AE}{Rg(\alpha)} - 2.315 - \frac{0.457 E_\alpha}{RT_\alpha}$$

where β is the heating rate; α is the conversion; T_α is the absolute temperature at the corresponding conversion; A is the pre-exponential factor; R is the gas constant; E_α is the activation energy at the conversion of a, and $g(\alpha)$ is the integral conversion function. For a fixed conversion, E_α is calculated from the slop of the fitting plot of $\log \beta$ *versus* $1000/T_\alpha$. In this work, the conversion values are chosen in the range from 25 to 65% where major degradation step is covered.

2.9 Grafting content calculation

The grafting process can be simply write as the following:

$$A + B = AB$$
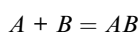
the residual mass of A, B and AB are a, b, c. While the grafting content A on B is x, the equation is true: $c = ax + (1 - x) b$.

3 Results and discussion

3.1 Characterization of the grafted antioxidants on the GO

GO and GO-RT were characterized by FTIR as shown in Fig. 2(a). Compared to GO, new peaks at 2921 cm^{-1} and 2853 cm^{-1} of –CH$_2$– associated with KH-560 appeared in the spectrum of GO-RT,[23] and new peaks at 1593 cm^{-1}, 1514 cm^{-1} and 1495 cm^{-1} were assigned to the characteristic peaks of benzene ring, demonstrating the successful grafting of RT.[24] Meanwhile, the absorption band related to epoxy groups (the peak of 956 cm^{-1}) in GO completely disappeared in the spectra of GO-RT due to the reaction between the epoxy groups and the amino groups. Hence, it can be concluded that RT had been successfully grafted onto the surface of GO.

Raman spectroscopy is a useful and convenient measurement to investigate the structures of carbonaceous materials,
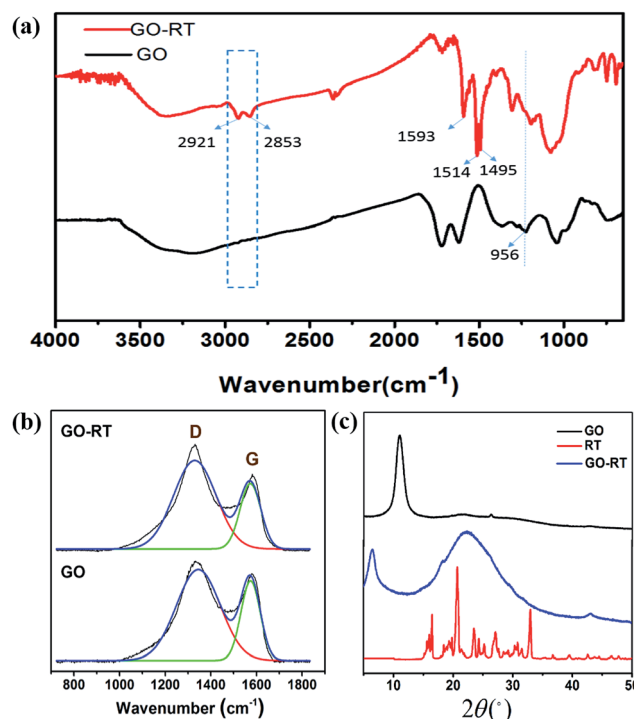

Fig. 2 FT-IR spectra (a), Raman spectra (b) and XRD curves (c) of GO and GO-RT.

especially for distinguishing ordered and disordered structures. Fig. 2(b) shows the Raman spectra for GO and GO-RT. Both of them had the D band at around 1340 cm^{-1} and G band at 1590 cm^{-1}. The D band is related to the vibration of sp^3 hybridized carbon and defects on the edges of GO formed during oxidation. The G band is derived from the vibration of sp^2 hybridized carbon in the graphite lattice.[23] The intensity ratio of D to G band (I_D/I_G) is often employed to evaluate the defects of graphene and monitor the functionalization of graphene. After grafting RT onto GO, the ratio of I_D/I_G increased from 1.158 to 1.313. This is because that the covalent functionalization increased the edge defects, resulting in the decrease of the average size of the sp^2 domain,[25,26] due to the grafted RT on the surface of GO. Furthermore, the XRD pattern of GO exhibited an obvious diffraction peak at $2\theta = 11.02°$, related to the oxygen-containing groups in GO;[23] while the GO-RT exhibited two diffraction peaks: the new diffraction peak at $2\theta = 22.42°$ was associated with the RT and the peak at $2\theta = 6.56°$ was owing to the GO, which had shifted, suggesting that there were chemical bonds between RT and GO, furthermore.

Subsequently, EDS was used to qualitatively analyze the element of GO and GO-RT. As shown in Fig. 3(a), only two significant peaks appeared in the GO spectra, which belonged to C and O; while new peaks of Si and N appeared in the GO-RT spectra, attributed by KH-560 and RT, respectively. The elements content of GO and GO-RT is shown in Fig. 3(a). It can be seen that the content of O decreased from 35.45% to 18.34%; while the content of N increased to 11.28%.

The TGA results of GO and GO-RT are shown in Fig. 3(b). It can be found that before 100 °C, the mass loss of GO was 4.4 wt%; while the mass loss of GO-RT only decreased to 1 wt%, indicating that grafting antioxidant can weaken the water-absorbing capacity of GO.[10] The change in the hydrophilicity of GO-RT confirmed the reaction between the oxygenic groups on the GO and the NH$_2$ bond on the RT. When the temperature heated up to 800 °C, the weight remaining of GO was 58.0 wt%, while the weight remaining of GO-RT decreased to 52.0 wt%. Therefore, the grafting content of RT on GO was determined to be 15.1%. Considering the loss of partial oxygen functionalities of GO in the process of reaction, it is reasonable that the grafting content of RT on GO is higher than 15.1%.
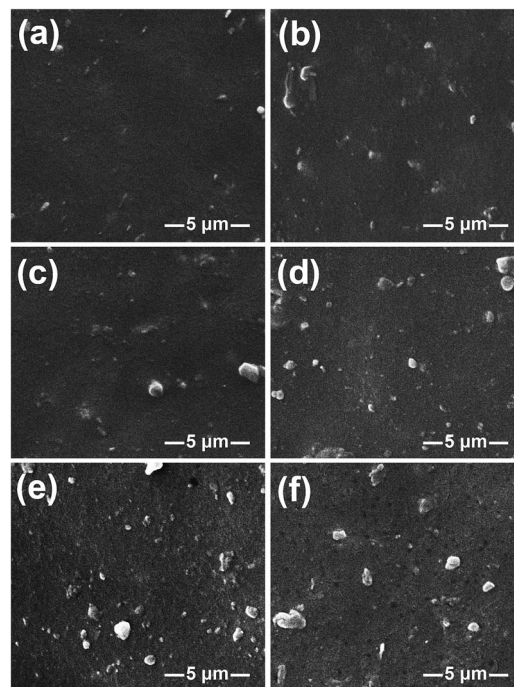

Fig. 4 SEM images of (a) SBR, (b) SBR/GO-RT(1), (c) SBR/GO-RT(2), (d) SBR/GO-RT(3), (e) SBR/GO-RT(4), (f) SBR/GO(4)/4010NA.

3.2 Morphology and dispersion of GO-RT in SBR matrix

The size and dispersion of GO and GO-RT in the composites was observed by SEM and the results are shown in Fig. 4. SBR is one kind of non-polar rubber, whereas the GO and GO-RT has a large amount of polar groups hydroxyl groups, carboxyl groups and epoxy groups, which leads to the aggregations of GO with large size due to low compatibility with SBR matrix.[27,28] As shown in Fig. 4(a–e), the dispersion became worse with the increase of GO-RT loading. However, compared with SBR/GO(4), the dispersion of GO-RT in SBR/GO-RT(4) composite was much better than GO in SBR/GO(4) composite as shown in Fig. 4(e) and (f), attributed to the decrease of oxygenic group of GO after grafting RT. Furthermore, the dispersion of antioxidant in SBR generally affects the mechanical property and antioxidant efficiency, which will be discussed in the following sections.
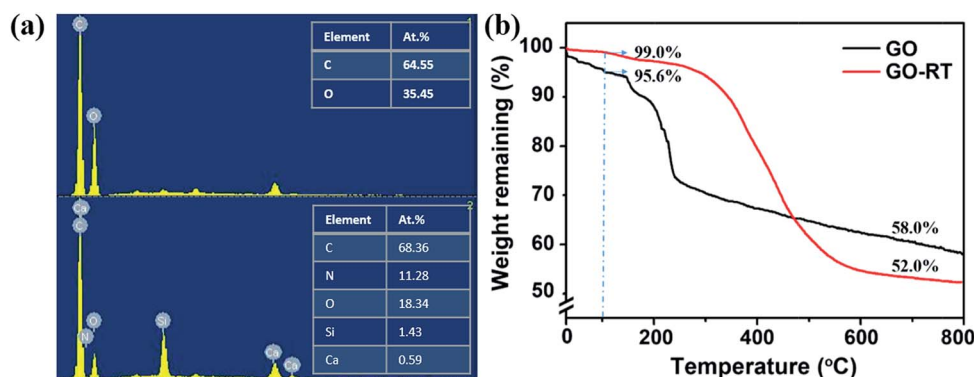

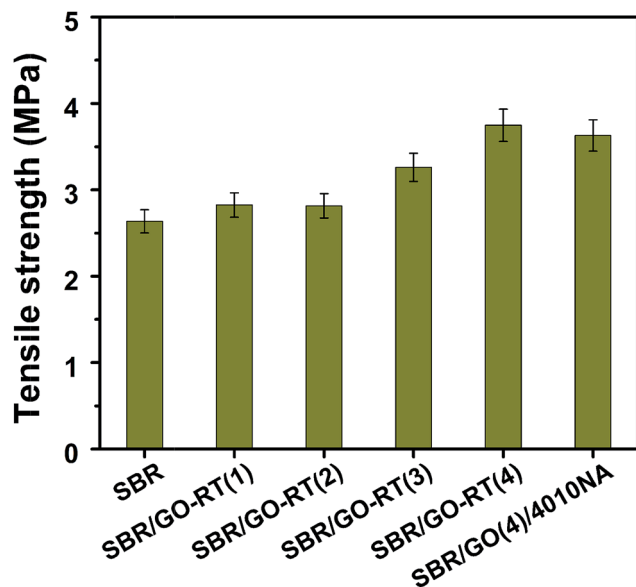Fig. 3 EDS spectra of GO and GO-RT (a) TGA curves of GO-RT and GO (b).

Fig. 5 The tensile strength of SBR composites.

3.3 The mechanical properties

According to the previous studies, the GO had positive effect on the mechanical property of rubber.[1,20] In the present study, the tensile strengths of SBR composites was evaluated and the results are shown in Fig. 5. It can be seen that the tensile strength of pristine SBR was 2.64 MPa, which was the lowest one; while the tensile strength of SBR composites was gradually improved with the increase of antioxidant loading, and the tensile strength of SBR/GO-RT(4) composite was 3.75 MPa, indicating that GO could enhance the tensile strength of SBR. Meanwhile, the tensile strength of SBR/GO-RT(4) was also higher than SBR/GO(4)/4010NA, which attributed to better dispersion of GO-RT than GO, corresponding to the observation of the SEM in Fig. 4.

3.4 The anti-oxidation efficiency of GO-RT in SBR matrix

The OIT test was utilized to evaluate the thermal oxidation resistance of SBR composites. OIT is the time interval between the initiation of oxygen flow and the onset of the oxidation reaction, which was commonly determined from the DSC curve.[17,29] It always used to estimate the stability of the composite material and the anti-aging efficiency of antioxidant. The longer the OIT is, the more efficient thermal oxidative property. The DSC curves and the OIT values of the SBR composites are shown in Fig. 6(a) and Table 2, respectively. It was found that the OIT A composite was 0 min, which was the lowest among the all kinds of SBR composites; while the OIT value of SBR composites gradually elevated with the increase of antioxidant loading, and the SBR/GO-RT(4) composite own the longest OIT which was about 40 min. The results indicate that GO-RT antioxidant had higher anti-aging efficiency than the low molecular weight antioxidant 4010NA.

To further evaluate the anti-aging performance of SBR composites, after different days' accelerated aging, the changes of mechanical property was investigated. The change tendency of the tensile strength of SBR composites during accelerated aging is presented in Fig. 6(b). In the process of accelerated aging, the tensile strength of pristine SBR and SBR composites had different degree of decline. However, the tensile strengths of SBR/GO-RT were always higher than that of pristine SBR. After aging for 12 days at 85 °C, the tensile strength of SBR/GO-RT(4) decreased to 2.79 MPa, which was still the highest among all the SBR composites, suggesting that the GO-RT had excellent anti-aging performance to remain the mechanical strength of SBR.
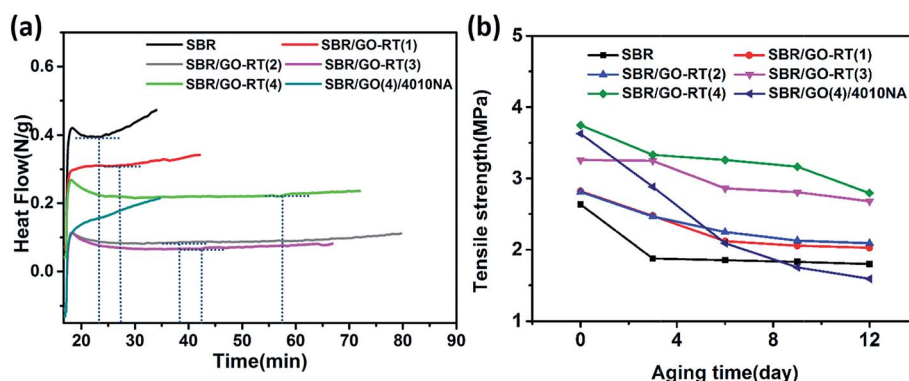

Fig. 6 (a) DSC curves of determining OIT (b) the changes of the tensile strength of SBR composites during accelerated aging.

Table 2 The OIT values of SBR composites

Sample	SBR	SBR/GO(4)/4010NA	SBR/GO-RT(1)	SBR/GO-RT(2)	SBR/GO-RT(3)	SBR/GO-RT(4)
OIT(min)	6	0	11	20	25	40

Table 3 Calculated activation energy by Flynn–Wall–Ozawa method

| Conversion | Pristine SBR | Activation/kJ mol^{-1} | | | | |
		SBR/GO-RT(1)	SBR/GO-RT(2)	SBR/GO-RT(3)	SBR/GO-RT(4)	SBR/GO(4)
25%	493.3822	625.7149	702.724	722.5539	757.611	706.815
35%	459.344	569.5909	636.8851	675.7263	700.9412	684.2522
45%	445.0992	533.2967	617.5828	670.6142	667.0302	685.7391
55%	443.4618	502.0419	639.141	658.0795	694.8466	700.6322
65%	409.0597	500.9503	673.1975	688.3701	777.3135	762.49
Average	450.0694	546.3189	653.9061	683.0688	719.5485	707.9857

mechanism of SBR. The average of activation of SBR/GO-RT(4) was higher than SBR/GO(4), even the conversion reached to 65%, which was caused by better thermal stability of GO-RT than GO.

4 Conclusions

Antioxidant functionalized graphene oxide (GO-RT) was successfully fabricated by grafting reactive antioxidant (RT) onto GO, which was confirmed by FT-IR, TGA, EDS and Raman spectra. It has been demonstrated that the GO-RT can effectively enhance the anti-aging efficiency of SBR and GO-RT existed anti-migration performance. In addition, the GO-RT can also enhance the mechanical properties of SBR. Thus, the excellent anti-aging property of the GO-RT could ensure long serve life of SBR.

Conflicts of interest

The authors declare that the research was conducted in the absence of any commercial or financial relationships that could be construed as a potential conflict of interest.

Acknowledgements

References

1 M. Tang, W. Xing, J. Wu, G. Huang, K. Xiang, L. Guo and G. Li, *J. Mater. Chem. A*, 2015, **3**, 5942–5948.

2 J. R. Shelton, *Rubber Chem. Technol.*, 1957, **30**, 1251–1290.

3 S. B. Munteanu, M. Brebu and C. Vasile, *Polym. Degrad. Stab.*, 2005, **89**, 501–512.

4 C. Xie, Z. Jia, D. Jia, Y. Luo and C. You, *Int. J. Polym. Mater.*, 2010, **59**, 663–679.

5 W. L. Hawkins, in *Polymer Degradation and Stabilization*, Springer, 1984, pp. 3–34.

6 O. Vogl, A. C. Albertsson and Z. Janovic, *Polymer*, 1985, **26**, 1288–1296.

7 F. Ignatz-Hoover, B. H. To, R. Datta, A. J. De Hoog, N. Huntink and A. Talma, *Rubber Chem. Technol.*, 2003, **76**, 747–768.

8 N. Ning, Q. Ma, Y. Zhang, L. Zhang, H. Wu and M. Tian, *Polym. Degrad. Stab.*, 2014, **102**, 1–8.

9 Q. Pan, B. Wang, Z. Chen and J. Zhao, *Mater. Des.*, 2013, **50**, 558–565.

10 H. Wei, J. Zhou, J. Zheng and G. Huang, *RSC Adv.*, 2015, **5**, 92344–92353.

11 Š. Chmela, P. Lajoie, P. Hrdlovič and J. Lacoste, *Polym. Degrad. Stab.*, 2000, **71**, 171–177.

12 N. Delaunay-Bertoncini, F. van der Wielen, P. De Voogt, B. Erlandsson and P. Schoenmakers, *J. Pharm. Biomed. Anal.*, 2004, **35**, 1059–1073.

13 M. Bertoldo and F. Ciardelli, *Polymer*, 2004, **45**, 8751–8759.

14 N. Haider and S. Karlsson, *Biomacromolecules*, 2000, **1**, 481–487.

15 S. Menichetti, C. Viglianisi, F. Liguori, C. Cogliati, L. Boragno, P. Stagnaro, S. Losio and M. C. Sacchi, *J. Polym. Sci., Part A: Polym. Chem.*, 2008, **46**, 6393–6406.

16 L. Guo, H. Lei, J. Zheng, G. Huang and G. Li, *Polym. Compos.*, 2013, **34**, 1856–1862.

17 X. Gao, G. Hu, Z. Qian, Y. Ding, S. Zhang, D. Wang and M. Yang, *Polymer*, 2007, **48**, 7309–7315.

18 B. Zhong, H. Dong, Y. Luo, D. Zhang, Z. Jia, D. Jia and F. Liu, *Compos. Sci. Technol.*, 2017, **151**, 156–163.

19 W. Xing, H. Li, G. Huang, L.-H. Cai and J. Wu, *Compos. Sci. Technol.*, 2017, **144**, 223–229.

20 X. Liu, W. Kuang and B. Guo, *Polymer*, 2015, **56**, 553–562.

21 J. Wu, W. Xing, G. Huang, H. Li, M. Tang, S. Wu and Y. Liu, *Polymer*, 2013, **54**, 3314–3323.

22 J. H. Flynn and L. A. Wall, *J. Polym. Sci., Part C: Polym. Lett.*, 1966, **4**, 323–328.

23 J. Bu, X. Huang, S. Li and P. Jiang, *Carbon*, 2016, **106**, 218–227.

24 V. Datsyuk, M. Kalyva, K. Papagelis, J. Parthenios, D. Tasis, A. Siokou, I. Kallitsis and C. Galiotis, *Carbon*, 2008, **46**, 833–840.

25 K. N. Kudin, B. Ozbas, H. C. Schniepp, R. K. Prud'Homme, I. A. Aksay and R. Car, *Nano Lett.*, 2008, **8**, 36–41.

26 S. Wolff and M.-J. Wang, *Rubber Chem. Technol.*, 1992, **65**, 329–342.

27 P. Sae-oui, C. Sirisinha, U. Thepsuwan and K. Hatthapanit, *Eur. Polym. J.*, 2007, **43**, 185–193.

28 I. Skjevrak, A. Due, K. O. Gjerstad and H. Herikstad, *Water Res.*, 2003, **37**, 1912–1920.

29 K. Thörnblom, M. Palmlöf and T. Hjertberg, *Polym. Degrad. Stab.*, 2011, **96**, 1751–1760.

30 A. Choudhury, A. K. Bhowmick, C. Ong and M. Soddemann, *J. Nanosci. Nanotechnol.*, 2010, **10**, 5056–5071.

31 S. Chen, H. Yu, W. Ren and Y. Zhang, *Thermochim. Acta*, 2009, **491**, 103–108.

32 K. Subramaniam, A. Das, L. Häußler, C. Harnisch, K. W. Stöckelhuber and G. Heinrich, *Polym. Degrad. Stab.*, 2012, **97**, 776–785.

33 M. Maiti, S. Mitra and A. K. Bhowmick, *Polym. Degrad. Stab.*, 2008, **93**, 188–200.